

# POLARIMETRIC SAR IMAGE SEGMENTATION USING TEXTURE PARTITIONING AND STATISTICAL ANALYSIS

Yongjian Yu and Scott T. Acton

Department of Electrical Engineering  
University of Virginia  
Charlottesville, VA 22903

## ABSTRACT

This paper presents a new technique for partitioning polarimetric synthetic aperture radar (POL-SAR) imagery into regions of homogeneous polarimetric backscattering properties. The method consists of two cascaded steps: an initial texture segmentation of one image derived from the POL-SAR data, and a polarimetric statistical region merging process that refines and modifies the initial segmentation. In the first stage, a morphological region-based image partitioning technique, the watershed algorithm, plays the key role. While in the second stage, the region adjacency graph and the segment dissimilarity measures derived from the Wishart model and the K distribution are applied. The overall segmentation algorithm has been tested using real 4-look POL-SAR imagery and sample results are provided in the paper. The main innovation of this work is the utilization of the K distribution in the segmentation process.

## 1. INTRODUCTION

Polarimetric SAR imagery facilitate the measurement of earth surface properties such as soil moisture, surface roughness, vegetation biomass, *etc.* The polarimetric approach improves upon such measurements taken by single polarization SAR imagery. For satellite-based polarimetric SAR remote sensing applications, there exists considerable interest in developing automatic data information extraction, content understanding and interpretation systems.

In an automated polarimetric SAR imagery content extraction and interpretation system, data segmentation is an important and essential first step. Simply stated, the goal of image segmentation is to partition the scene into disjoint, spatially connected, and homogeneous regions representing meaningful objects and background, with each region having uniform and similar polarimetric backscatter characteristics.

For fully polarimetric image segmentation, the maximum likelihood (ML) [1] and maximum *a posteriori* (MAP) [2] polarimetric classifiers have been proposed. Both techniques are based on the understanding of the statistics of the polarimetric data and upon multiple hypotheses testing. Single point statistics and spatial statistics are needed in the design of the ML and MAP classifiers, respectively. The multivariate complex Gaussian model [1] and the complex Wishart model [4] are two commonly used single point models; while the Markov random field (MRF) [2] model is a spatial model that makes use of both

the point polarimetric statistical model and contextual information of scene. The ML and MAP segmentation techniques in [1] and [2] are based on such models.

However, most of the ML techniques are performed on a pixel-by-pixel basis. Hence, such techniques are more akin to classification than segmentation. On the other hand, polarimetric K models [3] are generally believed to be more accurate than the Gaussian and Wishart in modeling of many varieties of textured natural objects [5]. Due to the lack of easily computable forms of distribution functions, however, the K model has not been used to implement ML or MAP segmentation of fully polarimetric SAR data.

In this paper, we attempt a new technique for fully polarimetric SAR image segmentation on a region-by-region basis. The method consists of two cascaded stages. The first stage is texture segmentation of the intensity image derived from the POL-SAR data, yielding an over-segmented initial segmentation. The second stage is a polarimetric statistics-based region merging. In the first stage, a watershed algorithm [6], [7] is used, while in the second stage an iterative merging technique is applied. The *region adjacency graph* representation is adopted to describe the relationship of initial and intermediate segments in the merging process. Segment dissimilarity measures are constructed from the Wishart model and the K models. Experimental results are provided.

## 2. DESCRIPTION OF THE ALGORITHM

The polarimetric data segmentation method consists of two distinct phases to be described below. The first phase produces an initial segmentation. And the second one proceeds the polarimetric statistics-based region merging.

### 2.1. Texture segmentation

First, a base image derived from the POL-SAR data is partitioned into its constituent regions in terms of texture features by applying the watershed transform [7] of the coefficient of variation map of the base image.

#### 2.1.1. Base image formation.

To facilitate the extraction of the underlying texture features for texture segmentation, a base image with sufficient speckle removal and sharpness is desirable. The span image is a non-coherent summation of HH, HV and VV polarized intensity images, namely,

$$span = |S_{hh}|^2 + 2|S_{hv}|^2 + |S_{vv}|^2. \quad (1)$$

In the span image, the speckle level is lower than in individual HH, HV or VV intensity images. As no spatial averaging is involved in its formation, the span image has the same high resolution as with the original data. The remaining speckle noise in the span image may still prohibit satisfactory texture segmentation; therefore, the sharpness-preserving morphological open-close filter with a fixed structuring element is applied to the span image to further reduce speckle level.

### 2.1.2. The Watershed algorithm

For optical images, the watershed algorithm is often performed on the gradient magnitude computed from the original image. The image is first mapped into a 3-D surface with gradient magnitude values being considered as altitudes. Segmentation is achieved by first locating and labeling the local minima within the surface. These local minima represent the *catchment basins* of the image. Each element of the surface is assigned to its corresponding catchment basin via a steepest descent path-following algorithm [8].

When applied to the gradient magnitude of an optical image, the boundaries in the resulting watershed segmentation correspond to the edges of regions in the original image. However, the gradient edge detectors based on the differences between pixel values usually fail in detecting edges in SAR images due to the presence of speckle noise. For SAR image segmentation, the coefficient of variation has been known to be a constant false alarm rate (CFAR) edge detector [9].

### 2.1.3. Edge detection

The coefficient of variation (CV) (i.e., the ratio of standard deviation to mean), is computed as the measure of the texture strength in the base image. Large CV values indicate the existence of edges. Hence, we can apply the watershed to an image of CV values.

## 2.2. Polarimetric statistic-based region merging

In the second stage, the initial texture segmentation is refined gradually toward the desired final polarimetric data segmentation by performing a hierarchical iterative polarimetric statistic-based region merging.

### 2.2.1 Statistic-based region merging process

The region merging process consists of five steps:

- (1) Perform connected component labeling of the initial segmentation.
- (2) Create a region adjacency graph (RAG) [10] for segments.
- (3) For each segment, consider the adjacent segments and identify the similar neighbors (unilateral similarity).
- (4) For segment pairs that are similar to each other (bilateral similarity), merge the segments and update the label map and the RAG.
- (5) Repeat steps (3) to (4) until desired segmentation is achieved.

In the RAG representation of segments, a node or vertex represents a segment and an edge (or arc) represents adjacency

between two nodes connected by an edge. Each node has associated relevant properties of the region it represents.

### 2.2.2. Multi-look polarimetric SAR image model

For a reciprocal medium ( $E_{hv} = E_{vh}$ ), the 1-look polarimetric data set can be represented by the transposed vector:

$$\underline{u} = [E_{hh} \quad E_{hv} \quad E_{vv}]^T. \quad (2)$$

The multi-look polarimetric data can be represented either by the Mueller matrix, the Stokes operator, or the covariance matrix.

Assume that the multi-look processed polarimetric SAR data are represented in the form of the covariance matrix,  $\underline{Z}$ , i.e.,

$$\underline{Z} = \frac{1}{n} \sum_{k=1}^n \underline{u}(k) [\underline{u}(k)]^T, \quad (3)$$

where  $n$  is the number of looks, and  $\underline{u}(k)$  is the  $k$ th 1-look sample.

We assume that the observed polarimetric SAR image  $\underline{Z}(x, y)$  is composed of distinct segments  $\{S_k\}$ , where each segment is viewed as a statistical population and is defined by its probability density function (PDF)  $f(\underline{Z}, \underline{\Sigma}_k)$  where  $\underline{\Sigma}_k$  is the 'ideal' unspeckled data.

For a homogeneous and texture-free region, the PDF of  $\underline{Z}$  is given by the Wishart distribution [4]:

$$f(\underline{Z}) = \frac{n^{3n} \|\underline{Z}\|^{n-3}}{R(n, 3) \|\underline{\Sigma}\|^n} \exp[-n \text{Tr}(\underline{\Sigma}^{-1} \underline{Z})], \quad (4)$$

in which  $R(n, 3) = \pi^3 \Gamma(n) \Gamma(n-1) \Gamma(n-2)$ ;  $n$  is the number of looks;  $\|\underline{Z}\|$  is the determinant of  $\underline{Z}$ ;  $\text{Tr}(\underline{\Sigma}^{-1} \underline{Z})$  denotes the trace of  $\underline{\Sigma}^{-1} \underline{Z}$ ;  $\underline{\Sigma} = E(\underline{Z})$ ; and  $\Gamma(x)$  is the gamma function.

It is well established that complex Wishart model does not provide a good description for textured land clutter because the basic assumptions associated with Wishart model generally do not hold in textured regions [3], [5]. A widely accepted statistical model for textured polarimetric SAR data is the so-called polarimetric K-model [5]. The K distribution arises as the result of underlying Gamma-distributed surface modulating the pure polarimetric speckle.

Let  $\underline{Y}$  represent the textured POL-SAR image. The K model for multi-look processed polarimetric SAR data is given by [3]:

$$f(\underline{Y}) = \frac{2 \|\underline{Y}\|^{n-3} (nv)^{(v+3n)/2} K_{v-3n}(2\sqrt{nv} \text{Tr}(\underline{\Sigma}^{-1} \underline{Y}))}{R(n, 3) \|\underline{\Sigma}\|^n \Gamma(v) (\text{Tr}(\underline{\Sigma}^{-1} \underline{Y}))^{-(v-3n)/2}}, \quad (5)$$

where  $K_\alpha(x)$  is the modified Bessel function of type two and of order  $\alpha$ , and  $\nu$  is the order parameter.

As the order parameter tends to infinity, the K distribution will approach Wishart model; as the order parameter tends to zero, the tail of the distribution lengthens so that the probability of very high intensity values becomes significant. This latter case provides a model for 'spiky' clutter scene such as encountered with imaging woodlands.

Based on the Wishart model and the K model, two polarimetric distance measures [4], [11] can be applied for classification of polarimetric SAR image on a pixel by pixel basis, i.e.,

$$d_1(\underline{Z}, \underline{\Sigma}) = \ln(\|\underline{\Sigma}\|) + \text{Tr}(\underline{\Sigma}^{-1} \underline{Z}). \quad (6)$$

and

$$d_2(\underline{Y}, n, \underline{\Sigma}) = \ln(K_{\nu-3n}(2\sqrt{n\text{Tr}(\underline{\Sigma}^{-1} \underline{Y})})) + 0.5(\nu - 3n) \ln(\text{Tr}(\underline{\Sigma}^{-1} \underline{Y})) + 0.5(\nu + 3n) \cdot \ln(n\nu) + n \ln(\|\underline{\Sigma}\|) - \ln(\Gamma(\nu)) - n \ln(\|\underline{Y}\|). \quad (7)$$

Note that metric  $d_1(\underline{Z}, \underline{\Sigma})$  is independent of the number of looks of the data; but  $d_2(\underline{Y}, n, \underline{\Sigma})$  depends on the number of looks.

### 2.2.3. Region dissimilarity measures

Let  $S = \{S_1, S_2, \dots, S_M\}$  be an M-partition of the image  $\underline{Z}(x, y)$ . According to the Wishart image model, the  $k^{\text{th}}$  homogeneous region is fully characterized by  $\underline{\Sigma}_k$ . The mean covariance matrices averaged over the region give the ML estimate of  $\underline{\Sigma}_k$ , namely

$$\underline{W}_k = \frac{1}{N_k} \sum_{(x,y) \in S_k} \underline{Z}(x, y), \quad (8)$$

where  $N_k$  denotes the cardinality of region  $S_k$ .

The objective cost function may be chosen as the error function:

$$E(S) = \sum_{k=1}^M \sum_{(x,y) \in S_k} d_1(\underline{Z}(x, y), \underline{W}_k). \quad (9)$$

Accordingly, it is inferred that the dissimilarity measure between the region  $S_i$  (under test) and its adjacent region  $S_j$  within Wishart distributed image is given by

$$C_{i,j} = \frac{N_i N_j}{N_i + N_j} d_1(\underline{W}_i, \underline{W}_j). \quad (10)$$

It is obvious to see that this criterion is not symmetric with respect to index  $i$  and  $j$ .

The dissimilarity measure between the region  $S_i$  (under test) and its adjacent region  $S_j$  in K-distributed images is given by

$$C_{i,j} = \frac{N_i N_j}{N_i + N_j} \left[ d_2(\underline{W}_i, nN_i, \underline{W}_j) + (nN_i - 3) \ln(\|\underline{W}_i\|) - \ln(\Gamma(nN_i) \Gamma(nN_i - 1) \Gamma(nN_i - 2)) \right]. \quad (11)$$

Due to the size weighting, the algorithm tends to merge regions of dissimilar size within the early iteration steps. If the dissimilarity metric is low, it means that the two regions share a common homogeneous region. The region merging process is iterated until a prefixed number of regions is obtained.

### 2.2.4. Distribution parameter estimation

In order to apply (11), the order parameter  $\nu$  needs to be selected. In our algorithm, this parameter is estimated using the single polarization sample data.

The order parameter may be estimated by [3]

$$(1 + 1/n)(1 + 1/\nu) = \langle t \rangle, \quad (12)$$

where  $\langle t \rangle$  is the average of the normalized intensity square over a uniform region,  $t = I^2 / \langle I \rangle^2$ ,  $I$  is any intensity. The estimator is appropriate when the value of  $\nu$  is large.

It has been established that the order parameter can be estimated more accurately for low order values by [12]

$$\text{var}[\ln(I)] = \psi'(\nu) + \psi'(n), \quad (13)$$

where  $\psi'(x)$  is the derivative of the digamma function  $\psi(x)$ . In comparison with (12), this method is more time-consuming, especially for large values of  $\nu$ .

As a compromise, (12) is first used to find an initial estimate of  $\nu$ . If this initial value is high ( $>5$ ), the estimate is accepted; otherwise (13) is used to refine the estimate.

Table 1 shows some estimated values of the order parameter in 4 selected areas, which are shown as numbered boxes in Fig. 1.

Table 1. Typical order parameter estimates

Order	Area 1	Area 2	Area 3	Area 4
$\hat{\nu}$	1.61	1.74	2.25	12.5

## 3. EXPERIMENTS AND RESULTS

The proposed algorithm has been tested to partition SIR-C L-band 4-look SAR images of Kowloon area, Hong Kong, as shown in Fig.1. The size of the image shown is 500 by 500 pixels. The initial segmentation from the watershed (shown in Fig.2) contains more than 800 segments. Before performing the fully polarimetric statistic-based region merging process, an intermediate region merging process is obtained in order to reduce the time of computation. The input data to this intermediate process are the logarithms of three diagonal

elements in  $\underline{Y}(x, y)$ . After the logarithmic transform, the speckle noise is transformed into additive noise homomorphically. The merging criterion is simply an Euclidean metric, *i.e.*, the square root of the summation of squared mean differences (in the logarithmic domain) between segments weighted by the same size factor as in Eq.(10) or (11). This distance measure is motivated by previous work on the estimation of single point statistics, which states that it is preferable to attempt the estimation process in the logarithm of the intensity for small sample [12]. Figure. 3 shows the results of this intermediate merging process.

Fig. 4 and Fig. 5 illustrate the further refinement of the watershed segmentation by way of the polarimetric statistic-based region merging process. In both figures, agreement is observed between the refined segments and different actual surface objects that can be identified visually in the span image.

#### 4. REFERENCES

- [1] J.A. Kong, A. A. Swartz, H.A. Yueh, L.M. Novak *et al.*, "Identification of terrain cover using the optimum polarimetric classifier," *J. of Electrom. Waves and Applications*, vol. 2, pp. 171-194, 1998.
- [2] Eric Rignot and Rama Chellappa, "Segmentation of polarimetric synthetic aperture radar data," *IEEE Trans on Image Processing*, Vol. 1, No. 3, July 1992, pp. 281—300.
- [3] J.S. Lee, D.L. Schuler, R. H. Lang, K. J. Ranson., "K-distribution for multi-look processed polarimetric SAR imagery," *IGARSS'94*, vol. 4, pp.2179-2181, 1994.
- [4] J.S. Lee, M.R. Grunes, T.L. Ainsworth, L. Du, *et al.*, "Unsupervised classification using polarimetric decomposition and complex Wishart classifier," *Proceedings to IGARSS'98*, Vol. 4, pp. 2178—2180, 1998.
- [5] David Blacknell and Alan P. Blake, "Single point and spatial statistics of polarimetric SAR imagery," *IEE Colloquim of Polarization in Radar*, pp. 1/1—1/9, 1996.
- [6] Benoit Ogar, Veronique Haese-coat and Joseph Ronsin, "SAR image segmentation by mathematical morphology and texture analysis," *Proceed. of IGRASS'96*, vol. 1, 1998.
- [7] F. Meyer and S. Beucher, "The morphological approach to segmentation: the watershed transformation," *Mathematical Morphology in Image Processing* (New York: Marcel Dekker, Inc.), pp. 433-481, 1992.
- [8] J.M. Gauch and S.M. Pizer, "Multiresolution analysis of ridges and valleys in grey-scale images," *IEEE Trans. on pattern Analysis and Machine Intelligence*, vol. 15, no.6, 1993.
- [9] R. Touzi, A. Lopes, and P. Bousquet, "A statistical and geometrical edge detector for SAR images," *IEEE Trans. On GRS.*, vol. 26, No. 6, Nov. 1988.
- [10] Kari Saarinen, "Color image segmentation by a watershed algorithm and region adjacency graph processing," *Proc. of the IEEE International Conference on Image Processing*, Austin Texas, November 1994.
- [11] J.S. Lee and Mitchell R.Grunes, "Classification of multilook polarimetric SAR data based on complex Wishart distribution", *Telesystems Conference, NTC-92, USA*, pp.7/21-7/24, 1992.
- [12] D. Blacknell, "Comparison of parameter estimators for K-distribution," *IEE Proc. -Radar, Sonar Navig.*, vol. 141, no. 1, Feb. 1994.

Fig. 1 Span image (Hong Kong)

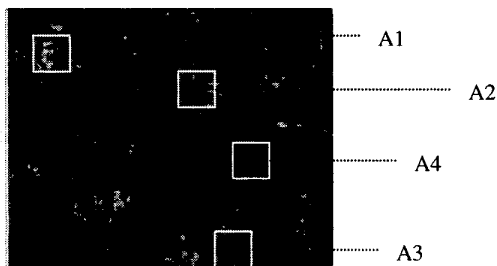


Fig. 3 Intermediate result 1

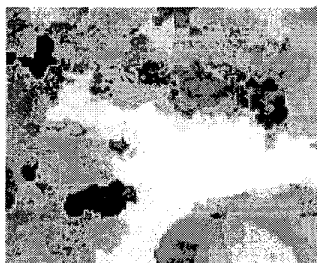


Fig. 4 Intermediate result 2

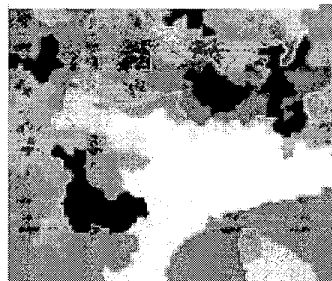


Fig. 2 Watershed segmentation

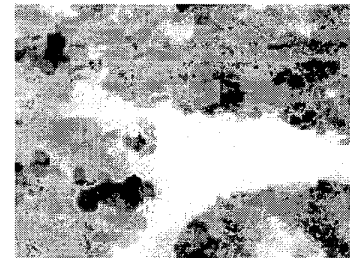


Fig. 5 Final result

